Bull. Mater. Sci., Vol. 38, No. 6, October 2015, pp. 1479–1486. © Indian Academy of Sciences.

Influences of protective atmosphere on the characterization and properties of $NaSr_2Nb_5O_{15}$ lead-free piezoelectric ceramics by sol–gel method

TIAN-HANG ZHANG, YAN-GAI LIU*, JIN-QIU ZHAO, ZHAO-HUI HUANG and MING-HAO FANG

School of Materials Sciences and Technology, China University of Geosciences (Beijing), Beijing 100083, China

MS received 20 June 2014; accepted 30 July 2015

Abstract. **$NaSr_2Nb_5O_{15}$ lead-free piezoelectric ceramics were prepared by the sol–gel method; they were sintered at different temperatures with or without protective atmosphere. The influences of sintering temperature and protective atmosphere on the characterization and properties of the ceramics were investigated. All the ceramics showed the pure tungsten bronze structure and an intermediate relaxor-like behaviour between normal and ideal relaxor ferroelectrics according to the modified Curie–Weiss law. The sintering temperature affected significantly the properties of ceramics, with the sintering temperature increased both with and without protective atmosphere, the ε_r, d_{33}, K_p and P_r of these ceramics initially increased and decreased finally, whereas the variation of Q_m and E_c showed the opposite tendency. Furthermore, the protective atmosphere also significantly affected the properties of these ceramics, ε_r, d_{33}, K_p and P_r of such ceramics sintered with protective atmosphere were superior to those of the ceramics sintered without protective atmosphere, while the tan δ, Q_m and E_c gave the contrary results.**

Keywords. **Sol–gel processes; protective atmosphere; dielectrics; ferroelectrics; piezoelectrics.**

1. Introduction

In the 21st century, environmental protection has been critically concerned. In 2003, the European Union classified lead as a hazardous substance and claimed that lead should be substituted. Now, more and more proponents research into lead-free piezoelectric ceramics.[1] Their enthusiasm particularly focusses on the preparation methods and properties of BT-based ceramics,[2] BNT-based ceramics,[3] KNN-based ceramics,[4] tungsten bronze-structured ceramics[5] and bismuth layer-type ceramics.[6] Among these lead-free piezoelectric ceramic systems, tungsten bronze-structured ceramics have received considerable attention owing to their superior dielectric,[7] piezoelectric[8,9] and ferroelectric properties.[10] The tungsten bronze-structured materials have a chemical formula of $(A_1)_2(A_2)_4(C)_4(B_1)_2(B_2)_8O_{30}$. In their crystal lattice structure, the A_1 and A_2 sites are, respectively, the 15- and 12-fold coordinated oxygen octahedral sites, which can be occupied by Na^+, K^+, Ca^{2+}, Sr^{2+}, Ba^{2+} and some rare earth cations. The C site is the 9-fold coordinated oxygen octahedral site and it can be occupied by Li^+ and other small cations. The B_1 and B_2 sites are the 6-fold coordinated oxygen octahedral sites and it can be occupied by either Nb^{5+} or Ta^{5+}. The smallest C site is often empty. Consequently, the formula $(A_1)_2(A_2)_4(B_1)_2(B_2)_8O_{30}$ is used for those filled tungsten bronze-structured variants[11,12] with the representative of $NaSr_2Nb_5O_{15}$ ceramics.

Unfortunately, it is difficult to prepare $NaSr_2Nb_5O_{15}$ ceramics with outstanding properties by using traditional solid-state methods. Although spontaneous polarization is limited in the presence of random grain characteristics,[13] other preparation methods of ceramic powders can overcome this limitation to enhance the properties of ceramics, i.e., the molten salts methods,[14] hydrothermal methods[15] and sol–gel methods.[16,17] In addition, the sol–gel methods attract more research attentions because the material compositions are controlled by molecular precursors. The mixing and reaction processes of metal organic complexes act at a molecular-scale, promoting a homogeneous product composition.[18] In the process of ceramics preparation, in order to obtain suitable properties, another key point is to control Na/Sr ratios in such ceramics. Obviously, $NaSr_2Nb_5O_{15}$ ceramics sintered in air resulted in Na vacancy as well as oxygen vacancy due to the evaporation of Na_2O.[19] Until now, the effects of excesssive $NaCO_3$ in raw material properties of lead-free piezoelectric ceramics were widely studied,[20] but the influences of protective atmosphere were seldom reported. Therefore, it is necessary to explore the relationship between protective atmosphere and properties of lead-free piezoelectric ceramics.

In the present work, the $NaSr_2Nb_5O_{15}$ lead-free piezoelectric ceramics were prepared by the sol–gel method and these were sintered at different temperatures with or without protective atmosphere. The differences of the ceramics sintered with or without protective atmosphere in the relative density and structure were also analysed. The influences of sintering

*Author for correspondence (liuyang@cugb.edu.cn)

temperature and protective atmosphere on the characterization and properties of these ceramics were investigated.

2. Material and methods

Niobium oxide (Nb_2O_5, 99.99%) was dissolved in the hydrofluoric acid (HF, 40%) followed by the addition of ammonium oxalate ($(NH_4)_2C_2O_4$, AR) and aqueous ammonia ($NH_3{\cdot}H_2O$, 28%) to form an $Nb(OH)_5$ deposit at a pH of 10. Next the $Nb(OH)_5$ deposit, sodium carbonate (Na_2CO_3, 99.99%), and strontium carbonate ($SrCO_3$, 99.99%) were added, respectively, to a citric acid ($C_6H_8O_7{\cdot}H_2O$, AR) solution, and injected with $NH_3{\cdot}H_2O$ to adjust the pH to 7. Ethylene glycol (AR) was added as an esterifying agent, which was subsequently dispersed by polyethylene glycol. The sol was initially presented after heating and mixing at 80°C and finally the gel formed by maintaining these conditions for 12 h: the gel was then dried at 120°C to obtain the precursor. The $NaSr_2Nb_5O_{15}$ powders were acquired after their precursors had been calcined at 1300°C for 6 h in air. In addition, the synthesized powders were compacted to discs with the diameter of 10 mm and the thickness between 1.0 and 1.5 mm under a pressure of approximately 120 MPa. Finally ceramics were obtained through sintering in the temperature range between 1275 and 1350°C with the temperature interval of 25°C for 6 h. The two sintering schemes were chosen in the sintering process of ceramics for comparison: the method of double enclosed alumina crucibles, in which ceramics were kept in a crucible surrounded by atmospheric powders of $NaSr_2Nb_5O_{15}$ (some atmospheric powders were shared between the double crucibles), and a single enclosed alumina crucible method in which atmospheric powder was not used. The sintered ceramics were lapped and electroded with a low-temperature silver paste by firing at 550°C for 30 min. The ceramics for piezoelectric property measurement were polarized in a silicone oil bath at 120°C by applying a DC electric field of 3 kV mm^{-1} for 30 min and then aged for 24 h.

The density was measured by Archimedes' method. The quantitative analyses were performed by an inductively coupled plasma optical emission spectrometer (ICP-OES, IRIS Intrepid II XSP, Thermo., USA). The phase structures of these ceramics were analysed by X-ray diffractometry (XRD, XD-3, Beijing, China) using Cu Kα radiation ($\lambda = 1.5406$ Å) with the 2θ range from 20° to 60°. The microstructures of surfaces and fracture surfaces were characterized by scanning electron microscopy (SEM, JSM-6469LV, JEOL, Japan) and the mean grain size was calculated by the line-intercept method. The dependences of dielectric property on temperature were measured by a multi-frequency inductance capacitance resistance (LCR) analyser (Agilent E4980A, Santa Clara, CA, USA), with an automated temperature controller, by measuring capacitance C and dielectric loss (tan δ) from room temperature to 350°C at 10 kHz, 100 kHz and 1 MHz. The piezoelectric constant d_{33} was measured with a quasi-static d_{33} measuring instrument (ZJ 3AN, Institute of Acoustics, Academic Sinica, China). The electromechanical coupling coefficient K_p and the mechanical quality factor Q_m were determined according to the resonance–antiresonance method based on IEEE standards with a precision impedance analyser (4294A, Agilent Technologies, Santa Clara, CA, USA). The polarization *vs*. electric (P–E) hysteresis curves were measured at room temperature using a precision materials analyser (Premier II, Radiant Technologies Inc., Albuquerque, NM, USA).

3. Results

The Na/Sr ratio was confirmed by ICP-OES analysis, as shown in figure 1. As the sintering temperature increased, the loss of strontium was slight, but the loss of sodium was larger. The Na/Sr ratios decreased with the increase in sintering temperature for the ceramics sintered with or without protective atmosphere and the loss of sodium in the ceramics sintered without protective atmosphere was higher than that in the ceramics sintered with protective atmosphere at the same temperature.

The X-ray diffraction patterns of the $NaSr_2Nb_5O_{15}$ ceramics sintered with or without atmospheric powder over the 2θ range from 20° to 60° are shown in figure 2a and b, independently. When the protective atmosphere was not used, the ceramics sintered at 1275, 1300, 1325 and 1350°C showed the pure tungsten bronze structure and no second phase could be detected (figure 2a). The ceramics sintered in the temperature range between 1275 and 1350°C and with the temperature intercal of 25°C also showed a pure tungsten bronze structure when the atmospheric powder was used during the sintering process (figure 2b).

Figure 3 shows the relative density (RD) as a function of temperature for ceramics sintered with or without protective atmosphere. RD is calculated based on the theoretical density of $Sr_2NaNb_5O_{15}$ (5.038 g cm^{-3}).[21] With the increase of sintering temperature, the relative density of the ceramics sintered without protective atmosphere initially increased rapidly and then its increase rate became more slow, the

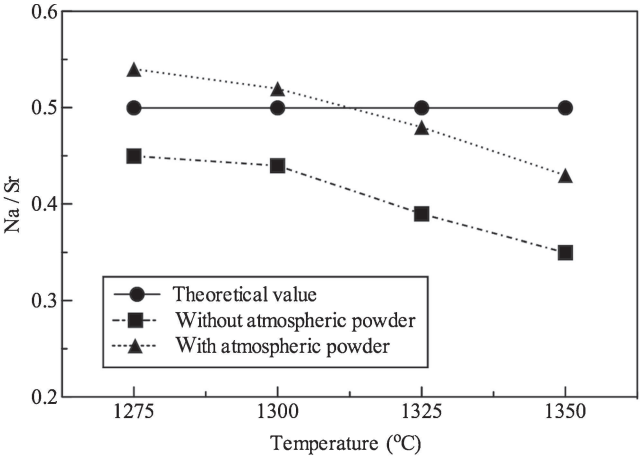

Figure 1. Results of ICP-OES analysis of $Sr_2NaNb_5O_{15}$ ceramics.

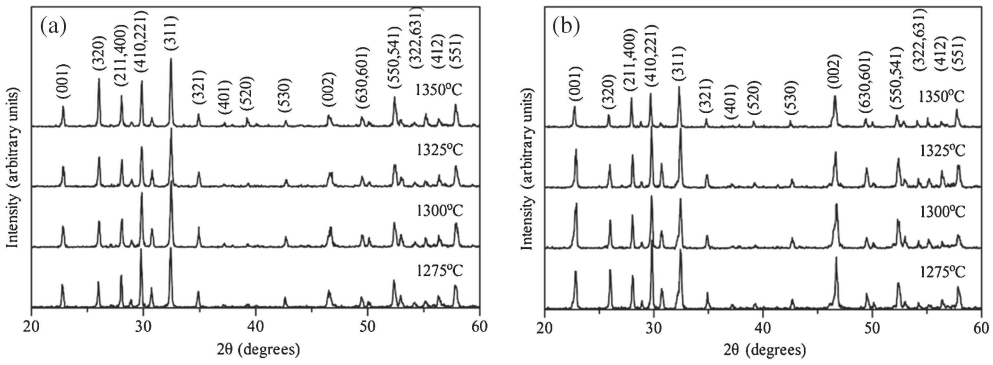

Figure 2. X-ray diffraction patterns of the $Sr_2NaNb_5O_{15}$ ceramics sintered at different temperatures: (**a**) without atmospheric powder and (**b**) with atmospheric powder.

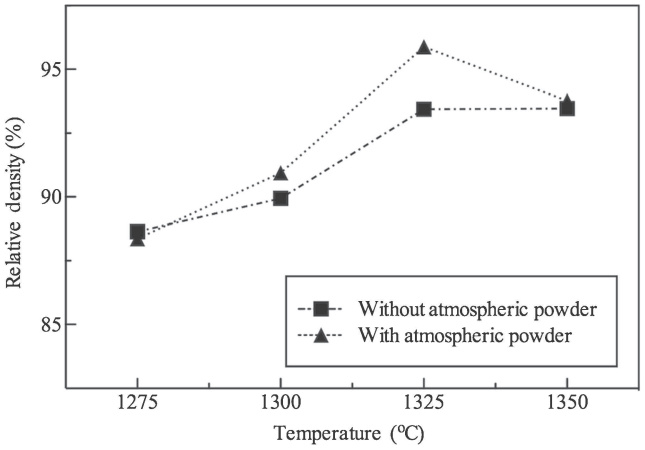

Figure 3. Relative density as a function of reaction temperature for ceramics.

maximum relative density of ceramics was 93.47%, which was obtained at the sintering temperature of 1350°C. However, with the increase of sintering temperature, the relative density of the ceramics sintered with protective atmosphere initially increased and then decreased. Also ceramics sintered at 1325°C reached the highest relative density (approximately 95.88%).

Scanning electron micrographs of the surface and fracture surface for $Sr_2NaNb_5O_{15}$ ceramics sintered without and with protective atmosphere at different temperatures are shown in figure 4. In these ceramics, there is an inhomogeneous grain size distribution on the surface: the grains show a bimodal grain size distribution with big grains being surrounded by small grains. Taking figure 4c as an example, the average grain sizes of the big and small grains were, respectively, 43.2 and 7.7 μm. When the protective atmosphere was not used, ceramics can be well microstructured at the sintering temperature of 1350°C and the grain sizes increased generally. Compared with that, the ceramics sintered with protective atmosphere can be dense at the lower sintering temperature of 1325°C. However, it could be seen that molten areas and cracks appeared on the surface of $Sr_2NaNb_5O_{15}$ ceramics when the sintering temperature was higher than 1350°C (figure 4e).

Figure 5a and b shows the temperature dependence of relative dielectric constant ε_r and loss tangent tan δ on the frequency: both ε_r and tan δ decreased with the increase in the frequency over the temperature range. For example, ε_r values at the Curie temperatures for the ceramics at 10 kHz, 100 kHz and 1 MHz were, respectively, 1647, 1486 and 1430 (figure 5b). The values of tan δ indicated that the dissipation for all ceramics was low (at 3.0%) at room temperature. At T_c, tan δ was less than 10% for all ceramics, and then tan δ increased. Besides, there was a dielectric peak at high temperature. The dielectric properties of all $NaSr_2Nb_5O_{15}$ ceramics are shown in table 1. The values of ε_r was firstly enhanced and then decreased as sintering temperature increased. The maximum ε_r values for ceramics with or without protective atmosphere were, respectively, 1094 and 1304, which were obtained at 1325°C. The results were different from the data presented in figure 5 because the measured ceramics had been polarized.

Except for the change in dielectric properties, protective atmosphere also significantly affected the piezoelectric properties of $NaSr_2Nb_5O_{15}$ ceramics. Table 1 shows the changes in the piezoelectric strain constant d_{33}, piezoelectric voltage constant g_{33}, electromechanical coupling factor K_p and mechanical quality factor Q_m as a function of sintering temperature for ceramics sintered with or without protective atmosphere. To achieve a high piezoelectric transfer efficiency, the ceramics should have an improved K_p and Q_m. With the increase of the sintering temperature, d_{33}, g_{33} and K_p showed a similar trend consisting of an initial increase and a subsequent decrease while Q_m showed the opposite trend. The values of d_{33}, g_{33} and K_p of ceramics sintered with protective atmosphere were superior to those of the ceramics sintered without protective atmosphere. When protective atmosphere was used in the sintering process, the optimal values of d_{33}, g_{33}, K_p and Q_m, 86 pC N^{-1}, 14 Vmm N^{-1}, 28.9 and 747, respectively, were obtained at 1325°C, which was a promising material with a potentially high piezoelectric transfer efficiency.

Figure 6 shows the P–E hysteresis loops of $NaSr_2Nb_5O_{15}$ ceramics, measured under an electric field of approximately 30 kV cm^{-1} at room temperature. Figure 6a and b shows that all the P–E loops were slanted and well-saturated.

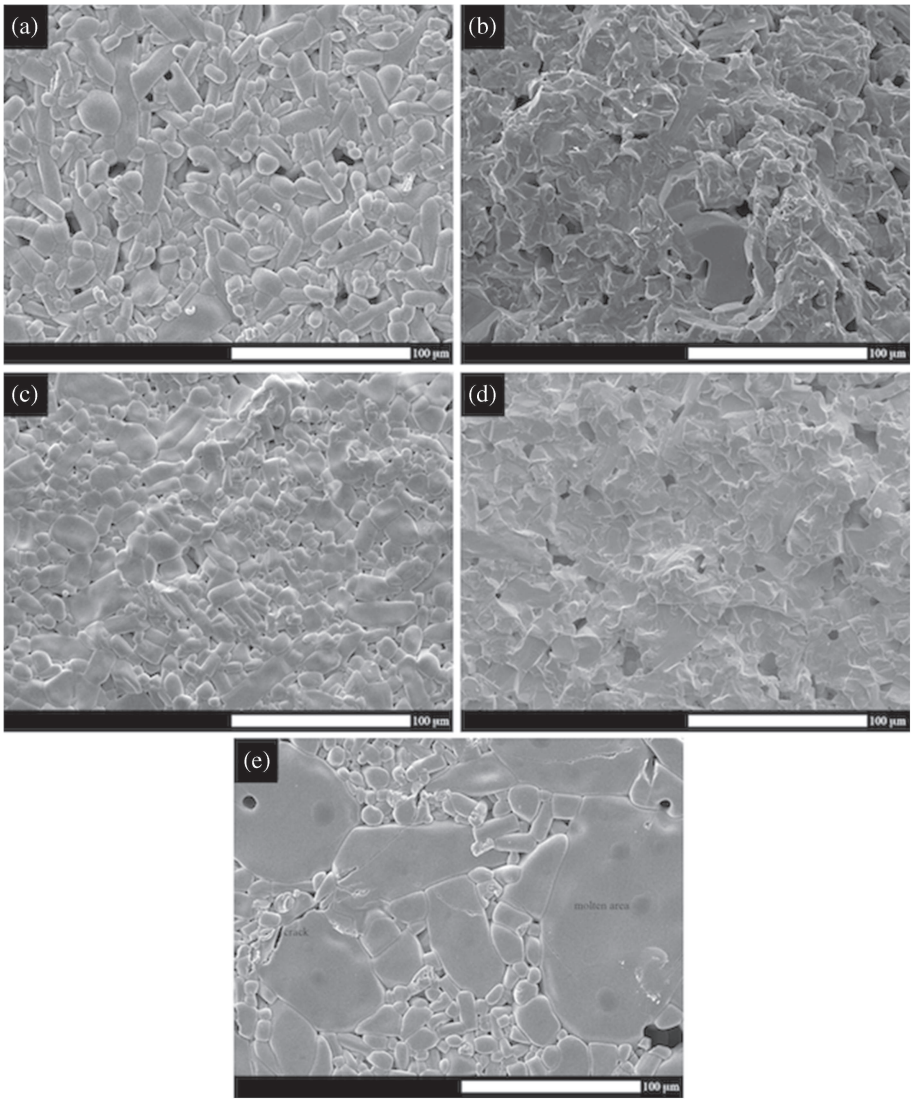

Figure 4. Scanning electron micrographs of the $Sr_2NaNb_5O_{15}$ ceramics: (**a**) surface, without atmospheric powder, at 1350°C, (**b**) fracture surface, without atmospheric powder, at 1350°C, (**c**) surface, with atmospheric powder, at 1325°C, (**d**) fracture surface, with atmospheric powder, at 1325°C and (**e**) surface, with atmospheric powder, at 1350°C.

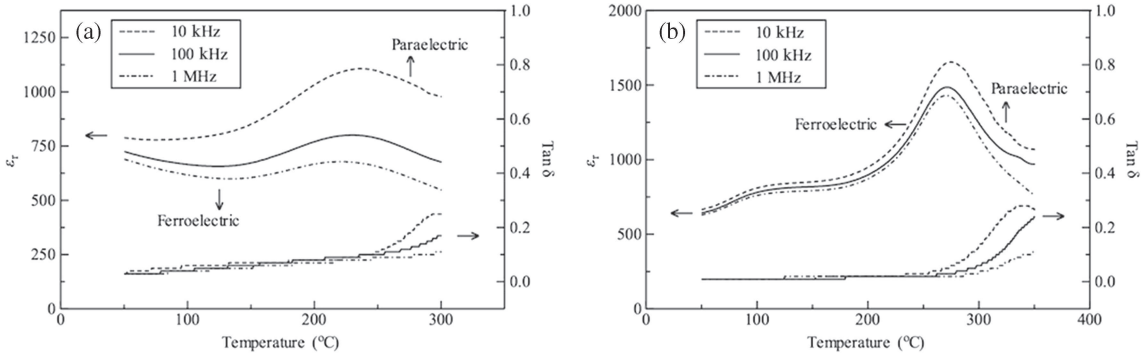

Figure 5. Temperature dependence of relative dielectric constant ε_r and loss tangent tan δ for $NaSr_2Nb_5O_{15}$ ceramics with different frequencies: (**a**) without atmospheric powder at 1325°C and (**b**) with atmospheric powder at 1325°C.

Table 1. Properties of $NaSr_2Nb_5O_{15}$ ceramics.

Temperature (°C)	RD (%)	T_c (°C)	ε_r^a	tan δ^a	E_c (kV cm^{-1})	P_r (μC cm^{-2})	P_s (μC cm^{-2})	d_{33} (pC N^{-1})	g_{33} (Vmm N^{-1})	K_p (%)	Q_m
Without atmospheric powder											
1275	88.64	—	786	0.022	19.21	12.81	15.39	49	7	21.7	1538
1300	89.95	—	813	0.025	18.04	14.64	18.88	48	6	22.1	1455
1325	93.45	221	1094	0.022	18.81	19.02	22.37	60	9	23.7	1206
1350	93.47	—	980	0.024	18.93	17.68	20.64	55	7	22.9	1330
With atmospheric powder											
1275	88.37	—	910	0.007	17.71	15.00	17.34	72	10	25.1	1085
1300	90.94	—	1169	0.008	16.05	18.23	21.37	76	12	27.6	868
1325	95.88	270	1304	0.008	15.92	18.81	23.43	86	14	28.9	747
1350	93.77	—	1249	0.009	17.43	18.63	22.01	80	11	25.9	1032

[a]Measured at room temperature, 1 MHz.

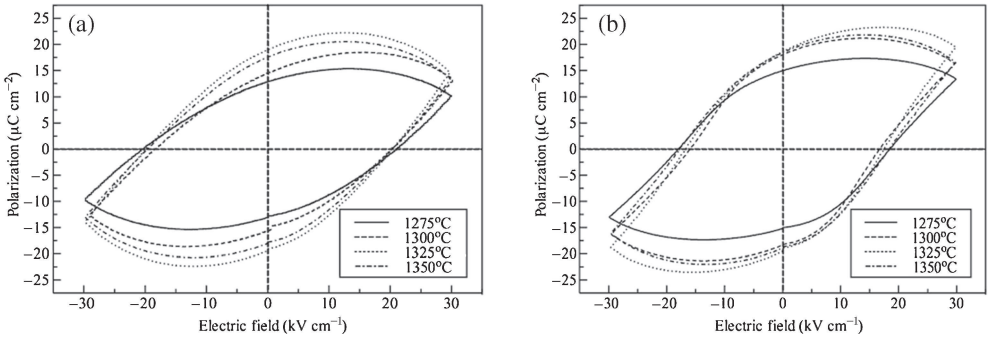

Figure 6. P–E hysteresis loops of the $NaSr_2Nb_5O_{15}$ ceramics measured at room temperature: (**a**) without atmospheric powder at 1350°C and (**b**) with atmospheric powder at 1325°C.

In figure 6a and b, spontaneous polarization P_s increased from 22.37 to 23.43 μC cm^{-2} and coercive field E_c decreased from 1.88 to 1.59 kV mm^{-1}. Compared with ceramics sintered without protective atmosphere, the $NaSr_2Nb_5O_{15}$ ceramics sintered with protective atmosphere had a lower E_c value and the relatively good ferroelectric properties. When protective atmosphere was used, the E_c decreased gradually when the sintering temperature increased from 1275 to 1325°C, and then started to increase and reached its minimum value of 1.59 kV mm^{-1} at 1325°C. The value of P_r increased from 15.00 to 18.81 μC cm^{-2} when the sintering temperature increased from 1275 to 1325°C and then decreased linearly when the sintering temperature was above 1325°C. The value of P_s showed a similar trend and reached its maximum value of 23.43 μC cm^{-2} at 1325°C.

4. Discussion

In $NaSr_2Nb_5O_{15}$ ceramics, the Na/Sr ratio as the quantity of Na^+ with the smaller ionic radius (r = 1.02 Å) to that of Sr^{2+} (r = 1.18 Å).[22] The evaporation of Na_2O was related to the melting point of the metallic oxides (1132°C for Na_2O, 2531°C for SrO and 1512°C for Nb_2O_5).[23] During the sintering process of ceramics, the evaporation of Na_2O from atmospheric powder can regulate the vapour phase equilibrium of Na_2O between the ceramics to be sintered and the atmospheric powder, in which the ceramics are embedded, thus reducing the evaporation of Na_2O from ceramics and maintaining the Na/Sr ratios. Although the Na/Sr ratios in the ceramics sintered with or without protective atmosphere were different, the best properties were achieved at 1325°C because the properties of ceramics also depended on the relative density. When sintering temperature of the ceramics sintered with protective atmosphere was 1325°C, the ceramics obtained excellent properties due to the near-theoretical Na/Sr ratio and density. When the sintering temperature increased from 1275 to 1350°C, the Na/Sr ratio of ceramics sintered without protective atmosphere decreased where as the relative density firstly increased and then was unchanged. Therefore, the optimal properties of the ceramics sintered without protective atmosphere were obtained at 1325°C.

The sintering process was described as follows. Firstly, the liquid phase was formed in the localized region with the high Na_2O concentration at high temperatures because Na_2O has low melting point of 1132°C. Then, the larger grains were obtained from dissolved small particles in the liquid. The liquid covered the surface of these grains and the density of ceramics was enhanced by liquid-phase sintering. When protective atmosphere was used, under the established

equilibrium of Na_2O vapour pressure between the $Sr_2NaNb_5O_{15}$ ceramics and $Sr_2NaNb_5O_{15}$ atmospheric powder, the evaporation of Na_2O was suppressed. In the final sintering stage, a majority of the liquid phase was re-absorbed into the grains. However, when protective atmosphere was not used in the sintering process, Na_2O flowed from the ceramics to the exterior, thus leading to the formation of Na_2O-rich phase in the grain boundary and ceramic surface. This was the reason why these ceramics sintered with protective atmosphere can be well microstructured at the lower sintering temperature of 1325°C. However, it could be seen that molten areas and cracks appeared on the surface of $Sr_2NaNb_5O_{15}$ ceramics when the sintering temperature was higher than 1350°C (figure 4e), indicating that ceramics were overheated. Abnormal grain growth (>100 μm), which was characterized by individual mega-grains embedded in a fine-grained matrix, was a phenomenon that often encountered in the sintering process of tungsten bronze-structured ceramics.[24] The liquid phase appeared at high sintering temperature due to the melting process of excessive Na_2O, forming a molten area. In these ceramics, the phase transition process happened at the Curie temperature, then the internal stress concentration was higher and sufficient to form cracks to release these stresses.[25] The existence of some molten areas and cracks could also explain the decrease in density of the $Sr_2NaNb_5O_{15}$ ceramic sintered at 1350°C (see figure 3).

In figure 5a and b, a dielectric peak at high temperatures corresponded to the phase transition from ferroelectric tetragonal (centrosymmetric) phase to paraelectric tetragonal (noncentrosymmetric) phase.[26] The relative dielectric constant of a normal ferroelectric material follows the Curie–Weiss law when the temperature surpasses T_c

$$\varepsilon_r = \frac{C}{T - T_o}(T > T_c), \tag{1}$$

where C is the Curie–Weiss constant and T_o is the Curie–Weiss temperature.[27] The variation of $1/\varepsilon_r$ with temperature for the $NaSr_2Nb_5O_{15}$ ceramics is shown in figure 7a and b. It was found that ε_r for ceramics deviated from the Curie–Weiss law over a wide temperature range above T_c, indicating that the ceramics had experienced a diffusion phase transition. The deviation from the Curie–Weiss law can be defined by ΔT

$$\Delta T = T_{cw} - T_c, \tag{2}$$

where T_{cw} is the temperature at which the curve starts to follow the Curie–Weiss law. The values of T_o, C, T_{cw} and ΔT for ceramics are presented in table 2. As shown in figure 7 and table 2, T_c is increased from 270°C for the ceramics sintered without protective atmosphere to 221°C for the ceramics sintered with protective atmosphere. T_{cw} increased in the presence of protective atmosphere, while ΔT decreased. The diffuseness of the phase transitions could also be explained by the modified Curie–Weiss law as follows:

$$\frac{1}{\varepsilon_r} - \frac{1}{\varepsilon_m} = \frac{(T - T_c)^\gamma}{C}, \tag{3}$$

where ε_m is the maximum value of the relative dielectric constant at the phase transition temperature,[28] γ and C were assumed to be constant (γ is the degree of diffuseness and C the Curie-like constant). The degree of diffuseness γ varies from 1 for a normal ferroelectric ceramic to 2 for an ideal relaxor ferroelectric ceramic. Plots of $\ln(1/\varepsilon_r - 1/\varepsilon_m)$ as function of $\ln(T - T_c)$ for ceramics between T_c and T_{cw} at the frequency of 1 MHz are shown in figure 8a and b. A linear relationship was observed in ceramics. The slope of the best-fit regression curves was used to determine γ. When protective atmosphere was not used in the sintering process,

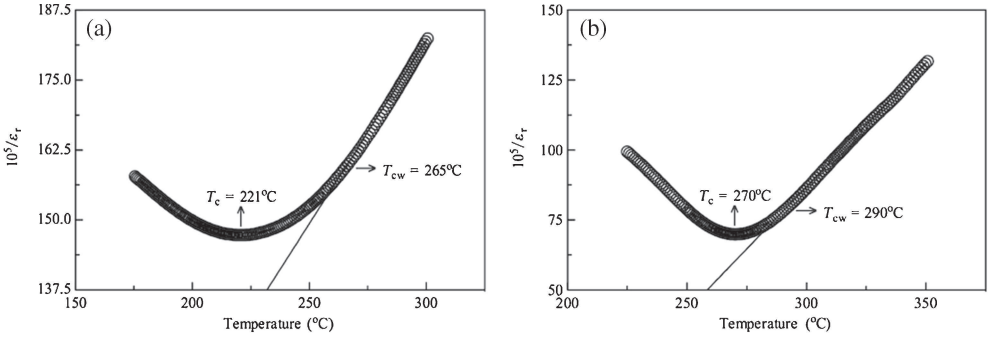

Figure 7. Variation of $1/\varepsilon_r$ with temperature in the $NaSr_2Nb_5O_{15}$ ceramics at 1 MHz: (**a**) without atmospheric powder at 1325°C and (**b**) with atmospheric powder at 1325°C. The symbols denote the experiment data, while the solid lines denote the least-squares fitting line to the modified Curie–Weiss law.

Table 2. T_o, C, T_{cw}, ΔT, ε_m and γ for $NaSr_2Nb_5O_{15}$ ceramics.

	T_o (°C)	T_{cw} (°C)	$C/10^5$ (°C)	ΔT (°C)	ε_m	γ
At 1325°C without atmospheric powder	21	265	1.5281	44	678	1.89
At 1325°C with atmospheric powder	201	290	1.1341	20	1430	1.71

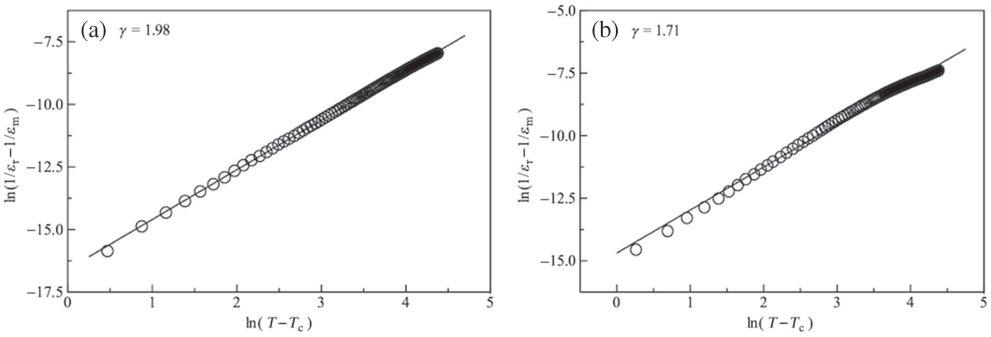

Figure 8. $\ln(1/\varepsilon_r - 1/\varepsilon_m)$ as function of $\ln(T - T_c)$ in the $NaSr_2Nb_5O_{15}$ ceramics at 1 MHz: (**a**) without atmospheric powder at 1325°C and (**b**) with atmospheric powder at 1325°C. The symbols denote experiment data, while the solid lines denote the least-squares fitting line to the modified Curie–Weiss law.

the larger γ-value of the ceramics suggested that the ceramics started to exhibit relaxor behaviour to a greater extent. When protective atmosphere was used, γ decreased from 1.89 to 1.71, indicating a reduction in the extent of relaxor behaviour. The interesting finding in the decrease of γ may be caused by the Na/Sr ratio of the ceramics, which tended to relaxor behaviour when the Na/Sr ratio deviated from its theoretical value.

The variations indicate that with the increase of the sintering temperature, the piezoelectric and ferroelectric properties of $NaSr_2Nb_5O_{15}$ ceramics is enhanced firstly and then weakened. The improved dielectric, piezoelectric and ferroelectric properties were reasonably attributed to the increase in density.[29] However, at high sintering temperatures, the loss of Na_2O was more obvious even the ceramics were sintered with protective atmosphere, thus weakening the dielectric, piezoelectric, and ferroelectric properties of ceramics. Although the ceramics sintered with or without protective atmosphere achieved the best dielectric, piezoelectric, and ferroelectric properties at the sintering temperature of 1325°C, the reasons were different. When the sintering temperature increased from 1275 to 1350°C, the Na/Sr ratios in the ceramics sintered without protective atmosphere decreased while the relative density in the such ceramics firstly increased and then was unchenged. Therefore, the optimal dielectric, piezoelectric, and ferroelectric properties the ceramics sintered without protective atmosphere were obtained at 1325°C. When sintering temperature of the ceramics sintered with protective atmosphere was 1325°C, the ceramics obtained excellent dielectric, piezoelectric and ferroelectric properties due to the near-theoretical Na/Sr ratio and density. The diminished E_c is due to the diminished grain boundary resulted from the density growth, thus preventing the polarization in the ceramics. Besides, the P–E hysteresis curves were unclosed because of the leakage current in the ceramics.[30,31] And the leakage in the P–E hysteresis loops of the ceramics prepared without protective atmosphere was more obvious because the relative density was low and the Na/Sr ratio deviated dramatically from its theoretical value and then the parameters derived from this P–E curves may not represent the true values. Therefore, $NaSr_2Nb_5O_{15}$ lead-free piezoelectric ceramics should be sintered with protective atmosphere

5. Conclusions

In this work, $NaSr_2Nb_5O_{15}$ lead-free piezoelectric ceramics were successfully prepared by the sol–gel method; they were sintered at different temperatures with or without protective atmosphere. According to the modified Curie–Weiss law, it is known that all these ceramics show an intermediate relaxor-like behaviour between the normal and ideal relaxor ferroelectrics. Protective atmosphere affects significantly the properties of ceramics because the ceramics sintered without atmospheric powder lose lots of sodium, as confirmed by the quantitative analyses. ε_r, d_{33}, K_p and P_r of such ceramics sintered with atmospheric powder were superior to those of the ceramics sintered without atmospheric powder, while the $\tan\delta$, Q_m and E_c gave the contrary results. Consequently, the properties of such ceramics sintered with atmospheric powder became more and more wonderful. Furthermore, sintering temperature also significantly affects the properties of ceramics because the relative density of ceramics is enhanced when sintering temperature is increased. With the sintering temperature increased both with and without atmospheric powder, the ε_r, d_{33}, K_p and P_r of these ceramics initially increased and decreased finally, while the variation of Q_m and E_c showed the opposite tendency. When the sintering temperature was 1325°C in the presence of protective atmosphere, the ceramics had a near-theoretical density and Na/Sr ratio and the outstanding material properties: RD = 95.88%, $T_c = 270$°C, $\varepsilon_r = 1304$, $\tan\delta = 0.008$, $E_c = 1.59$ kV mm^{-1}, $P_r = 18.81$ μC cm^{-2}, $P_s = 23.43$ μC cm^{-2}, $d_{33} = 86$ p N^{-1}, $g_{33} = 14$ V mm N^{-1}, $K_p = 28.9\%$ and $Q_m = 747$.

Acknowledgements

The financial support from the Fundamental Research Funds for the Central Universities (Grant no. 2012067) is gratefully acknowledged. We also thank the Program for New Century

Excellent Talents in University (Grant no. NCET-12-0951) and the New Star Technology Plan of Beijing (Grant no. 2007A080).

References

1. Qing Y and Li Y X 2011 *J. Adv. Dielectr.* **1** 269
2. Li W, Xu Z J, Chu R Q, Fuand P and Zang G Z 2011 *Mater. Sci. Eng. B: Solid* **65** 176
3. Lin D M and Kwok K W 2010 *J. Mater. Sci.: Mater. Electron.* **21** 291
4. Chen Z H, Qiu J F, Liu C, Ding J N and Zhu Y Y 2010 *Ceram. Int.* **36** 241
5. Fan X J and Wang Y 2011 *J. Syn. Cryst.* **40** 639
6. Wang K and Li J F 2010 *Adv. Funct. Mater.* **20** 1924
7. Auciello O, Scott J F and Ramesh R 1998 *Phys. Today* **51** 22
8. Neurgaonkar R R, Oliver J R, Copy W K, Cross L E and Viehland D 1994 *Ferroelectrics* **160** 265
9. Hao X and Yang Y F 2007 *J. Mater. Sci.* **42** 3276
10. Liu W C, Mak C L and Wong K H 2009 *J. Phys. D: Appl. Phys.* **42** 105
11. Garcia-Gonzalez E, Torres-Pardo A, Jimenez R and Gonzalez-Calbet J M 2007 *Chem. Mater.* **19** 3575
12. Ganguly P and Jha A K 2011 *Mater. Res. Bull.* **46** 692
13. Fang P Y, Fan H Q, Xi Z Z, Chen W X, Chen S C, Long W and Li X J 2013 *J. Alloys Compd.* **550** 335
14. Yang Z P, Wei L L and Chang Y F 2007 *J. Eur. Ceram. Soc.* **27** 267
15. Sheikhiabadi P G, Salavati-Niasari M and Davar F 2012 *Mater. Lett.* **71** 168
16. Zhang T H, Zhao J Q, Liu Y G, Huang Z H and Fang M H 2013 *Key Eng. Mater.* **544** 96
17. Gao G Z, Liu Y G, Huang Z H and Fang M H 2012 *Key Eng. Mater.* **492** 198
18. Wang C, Hou Y D, Ge H Y, Zhu M K and Yan H 2009 *J. Eur. Ceram. Soc.* **29** 2589
19. Hou Y D, Zhu M K, Wang H, Wang B, Tian C S and Yan H 2004 *J. Eur. Ceram. Soc.* **24** 3731
20. Wang Y, Zhang Y C, Hu Z J, Gao X, Guo X F and Jiang Y J 2009 *J. Beijing Univ. Technol.* **35** 125
21. Wei L L, Yang Z P, Gu R and Ren H M 2010 *J. Am. Ceram. Soc.* **93** 1978
22. Singh K C, Jiten C and Laishram R 2010 *J. Alloys Compd.* **291** 717
23. Yao Y B, Mak C L and Ploss B 2012 *J. Eur. Ceram. Soc.* **32** 4353
24. Lee H Y and Freer R 1998 *J. Mater. Sci.* **33** 1703
25. Li B R, Wang X H, Li L T, Zhou H, Liu X T and Han X Q 2004 *Mater. Chem. Phys.* **83** 23
26. Zheng M P, Hou Y D, Ge H Y, Zhu M K and Yan H 2013 *J. Eur. Ceram. Soc.* **33** 1447
27. Fan X J, Wang Y and Jiang Y J 2011 *J. Alloys Compd.* **509** 6652
28. Wei L L, Yang Z P, Gu R and Pan H 2011 *Mater. Chem. Phys.* **126** 836
29. Uchino K and Nomura S 1982 *Ferroelectrics* **44** 55
30. Zhao P, Zhang B P and Li J F 2007 *Appl. Phys. Lett.* **90** 2409
31. Wang Y L, Damjanovic D and Klein N 2007 *J. Am. Ceram. Soc.* **90** 3485